Celestial Mechanics and Dynamical Astronomy (2024) 136:39
https://doi.org/10.1007/s10569-024-10207-1

ORIGINAL ARTICLE

Spin orbit resonance cascade via core shell model: application to Mercury and Ganymede

Gabriella Pinzari[1] · Benedetto Scoppola[2] · Matteo Veglianti[2]

Received: 13 February 2024 / Revised: 15 July 2024 / Accepted: 19 July 2024 /
Published online: 10 September 2024

Abstract
We discuss a model describing the spin orbit resonance cascade. We assume that the body has a two-layer (core–shell) structure; it is composed of a thin external shell and an inner and heavier solid core that are interacting due to the presence of a viscous friction. We assume two sources of dissipation: a viscous one, depending on the relative angular velocity between core and shell and a tidal one, smaller than the first, due to the viscoelastic structure of the core. We show how these two sources of dissipation are needed for the capture in spin–orbit resonance. The shell and the core fall in resonance with different time scales if the viscous coupling between them is big enough. Finally, the tidal dissipation of the viscoelastic core, decreasing the eccentricity, brings the system out of the resonance in a third very long time scale. This mechanism of entry and exit from resonance ends in the $1:1$ stable state.

Keywords Tidal dissipation · Spin orbit resonance · Core shell model

1 Introduction

It is well-known that Hamiltonian mechanics is a very effective way to describe the astronomical motions because the systems are in this context almost conservative. However considering the fact that the bodies are extended, instead of point masses, and that their inner motions, mainly due to tides, dissipate energy, some small non-conservative effects have to be taken into account. More recently, the argument has been deeply studied, and it became very important also because we have today the possibility to perform astronomical measurements with an impressive precision. Actually, the main motivation of this work is to introduce an inter-

✉ Matteo Veglianti
veglianti@mat.uniroma2.it

Gabriella Pinzari
Gabriella.Pinzari@math.unipd.it

Benedetto Scoppola
scoppola@mat.uniroma2.it

[1] Dipartimento di Matematica "Tullio Levi-Civita", Università degli studi di Padova, Via Trieste, 63, 35131 Padua, Italy

[2] Dipartimento di Matematica, Università di Roma "Tor Vergata", Via della ricerca scientifica, 00133 Rome, Italy

pretative framework for the measurement of Ganymede by the space mission JUICE. Indeed the 3GM experiment will be able to measure with high accuracy the Ganymede's gravity field and the thickness of subsurface ocean, see Cappuccio et al. (2020). Both these measures can be related to the friction coefficients of our model, as we will show below. We want also to remind that recent space missions (JUICE, Juno, BepiColombo) are receiving considerable support frameworks in literature, consisting in both analytically and numerically models, see, for instance (Lari et al. 2022; Lari 2018).

The literature about tidal dissipation and triaxial effects is immense, see for instance (Murray and Dermott 1999; Efroimsky and Makarov 2013; Efroimsky 2015; Ferraz-Mello et al. 2015) and references therein. The subject is quite subtle, most of all because the friction appearing in this dissipation is a very complicated topic, and we have so far only phenomenological models of it. Just to quote a relatively recent development with this respect, in a geological framework the motion between plaques is supposed to exhibit the so-called stick/slip phenomenon, see for instance (Corbi et al. 2011). In order to acquire the possibility of a detailed control of the parameters of the system, an accurate description is needed, but it is still far from the current knowledge. Some attempt, in a statistical mechanics context, has been preliminary performed in terms of the so-called shaken dynamics, see for instance (Scoppola et al. 2022b; Apollonio et al. 2022a, b; D'Autilia et al. 2021; Apollonio et al. 2019), but the subject is really in a very primordial state.

On the other side, a quantitative control of the friction involved in the tidal phenomena could be very useful in order to study the numerous resonances that can be observed in solar system. In this paper, we will face a simple form of resonance, namely the rational ratio between the orbital period and the spin period; we will call this resonance *spin–orbit resonance*.

While it is definitely quite clear that such resonances may appear in celestial mechanics, see again for instance (Murray and Dermott 1999; Correia et al. 2018; Antognini et al. 2014; Scoppola et al. 2022a), it is much less clear, from a quantitative point of view, how it is possible that the systems are captured by certain resonances. An example particularly clear with this respect is the 3:2 spin–orbit resonance exhibited by Mercury. The latter has been investigated in pioneering works, see Goldreich and Peale (1966, 1967), and it has been immediately clear that the probability of capture in the observed resonance for Mercury is extremely small if one wants to describe the tidal friction in terms of simple phenomenological relations. After this first computations, various models have been proposed in order to overcome this difficulty, giving a more plausible justification of the observed resonance. Here, we want to recall the paper (Noyelles et al. 2014), in which the capture in resonance has been described in term of a very detailed and frequency dependent model of tidal friction. On the other hand, numerical approaches are also proposed, see, for instance (Bartuccelli et al. 2015; Correia and Laskar 2009, 2010).

For the physical reasons mentioned above, we believe that a description of the capture into resonance based on a detailed knowledge of the friction is not completely satisfying. Hence, following some ideas in Baland et al. (2019), Goldreich and Peale (1966), Goldreich and Peale (1967), in this paper, we propose a different model of the capture in resonance that we briefly describe here.

The basic idea is the following: Assume that the body is composed by a thin solid crust and an inner and heavier solid core, both triaxial, that are interacting due to the presence of a fluid interface. This interaction, when the rotations of the crust and the core are different, is a first source of dissipation. A second, much smaller, source of friction is due to the viscoelastic structure of the core, in which the tidal deformation is not completely elastic, implying a certain dissipation. In principle, a similar source of friction on the crust is also present, but

since it is reasonable to assume that it contributes with small effects and, in any case, it does not add anything to the general description, we will neglect this term for the sake of simplicity.[1] Other kind of interactions between core and crust, such as self-gravitational, pressure or electromagnetic, are sometimes considered in literature, for an exhaustive discussion see Rochester (1970). For the aim of this paper, we neglect all this kind of couplings that we implicitly suppose much smaller than the two we are considering.

We will face in the rest of the paper two different systems, namely Sun-Mercury and Jupiter-Ganymede. The structure described above is shared by these two systems, with an important difference: indeed, according to Juno's data, the liquid interface in the case of Ganymede is supposed to be composed of liquid water, see for instance (Gomez Casajus et al. 2022); Mercury, on the contrary has probably a molten mantle, exhibiting a viscosity about 7 order of magnitude higher than the water's, see for instance (Smith et al. 2012). In literature, it is possible to find some studies, related to different phenomena, starting from these assumptions on the inner structures of the celestial bodies, see for instance (Folonier and Ferraz-Mello 2017; Baland et al. 2019; Ragazzo et al. 2022).

In order to describe the two sources of dissipation in the system, we assume a simple viscous friction, linearly dependent on the difference of velocity, for the interaction between crust and core, i.e., similar to equation (10) in Correia and Laskar (2009). As it will be clear below, using a rough computation based on laminar solution of the Navier–Stokes equation, this assumption seems to be reasonable, and it is possible to give an estimate of the order of magnitude of the torque produced by this kind of friction. The description of the capture in resonance, anyway, is not dependent on this linearity assumption; we just need a continuous friction vanishing at zero velocity. The details about the viscoelastic friction on the core are even less important in order to achieve the results of this paper. The only important assumption with this respect is the fact that the viscoelastic tidal torque on the core has to be smaller than the viscous torque applied to the crust-core system. Rough estimates, see again next sections, show that this assumption is fulfilled in the two specific systems we are studying. Since the details of the viscoelastic torque on the core are inessential, we will describe it again in terms of a friction linear in velocity, in order to be able to write the equation of motions by means of a Rayleigh function.

As it will be clear below, the mechanism leading to the capture in spin–orbit resonance of the celestial bodies seems to be the following. The (much lighter) crust usually rotates jointly with the core. A viscoelastic tidal torque acting on the core is always present that slowly decreases the angular velocity of the whole body. When the angular velocity of such whole body becomes sufficiently close to a resonance the crust is certainly captured in resonance on a very small time scale. Then, if the contribution of the viscoelastic friction is sufficiently small with respect to the viscous coupling between crust and core, the core is driven, again with certainty, to the same resonance on a different and slightly longer time scale. The body, then, exits from resonance when the action of the viscoelastic torque reduces the eccentricity of the orbit under a certain limit value, and this happens on a third longer time scale. The whole process causes a cascade of spin–orbit resonances, bringing eventually the system in the stable 1:1 state.

For the seek of simplicity, we consider only the leading terms of expansions in the small parameters of the system. Future works will be devoted to the control of the convergence of such expansions following the approach presented in Chen and Pinzari (2021), Celletti and Chierchia (2000), Calleja et al. (2022). The work is organized as follows. In Sect. 2, to recall the mechanism leading to the spin–orbit resonance and to fix some notations, we present

[1] See below for numerical estimates.

the equations of motions of the two layers without viscous coupling. Then, we evaluate the stability of any generic spin–orbit resonance. In Sect. 3, we introduce the two dissipative terms, we discuss the capture mechanisms, and we find out a condition on the eccentricity that ensure the capture into spin–orbit resonance for the crust and the core. In Sect. 4, we show how the system exits from a resonance to go to the next one. Finally, Sect. 5 is devoted to some preliminary numerical computation and to the discussion of future developments of the work.

2 Stability of spin–orbit resonance

Celestial bodies such as Mercury or some of the Jovian satellites consist of several layers of materials with different density that interact differently with other celestial body (e.g., the Sun, Jupiter or the other satellites). The rotational velocity of such layers is, in general, not the same. It is reasonable to think that the friction between them depends on their mutual angular velocity.

In this framework, we introduce a simple model in order to compute the effects of inner dissipation in the two body problem. We want to investigate the effects that this dissipation has on the orbital evolution and in particular on the spin–orbit resonance capture. We will assume that the two bodies have very different masses, say $M \gg m$, and we call *central body* the body with mass M and *orbiting body* the body with mass m. To keep the model as simple as possible, we assume the axis of rotation of the orbiting body to be perpendicular to the orbital plane. Indeed both in the case of Mercury and Ganymede, the obliquity is negligible; Mercury has a very tiny obliquity and some recent papers show that Ganymede's obliquity is lesser than a degree, see, for instance (Hay and Matsuyama 2019).

In our model, we assume a three-layer structure of the orbiting body: an inner solid not perfectly elastic heavy core and an external solid thin and light crust, both described in terms of triaxial ellipsoid, separated by a fluid ocean (Ganymede) or a viscous mantle (Mercury). Following the idea in Baland et al. (2012, 2019) and Coyette et al. (2016), the ocean is divided into an inner part attached with the core and an outer part attached with the crust, the boundary between the two being a sphere with radius equal to the semi-major axis of the core, see Fig. 1. Then, we call *core* the interior part of the body, composed by the true core together with the inner part of the ocean and *shell* the external part of the body, composed by the outer part of the ocean together with the crust. So the orbiting body, centered in P, is described in terms of a core of mass $m-\mu$ and a not perfectly spherical shell of mass μ. Let A, B, C and A', B', C' be respectively the moments of inertia of the core and of the shell with respect to the reference axis. In particular, C and C' are the moments of inertia with respect to the spin direction. The equatorial ellipticity are therefore $\varepsilon = \frac{3}{2}\frac{B-A}{C}$ and $\varepsilon' = \frac{3}{2}\frac{B'-A'}{C'}$ respectively. It is reasonable to assume that the triaxiality shape of core and shell are similar: $\varepsilon \simeq \varepsilon'$; but, since the shell is lighter and thinner than the core, it is also reasonable to assume that each moment of inertia of the shell is smaller than the corresponding moment of inertia of the core, in particular $C' << C$.

The results we obtain remain unchanged if one considers a simpler model in which the orbiting body, centered in P, is described in terms of a not perfectly spherical core of mass $m-\mu$ and a mechanical dumbbell centered in P, i.e., a system of two points, each having mass $\mu/2$, constrained to be at fixed mutual distance $2l$, having P as center of mass. The idea is to substitute the triaxiality of the shell with a dumbbell. In this paper, however, we follow the first more usual approach.

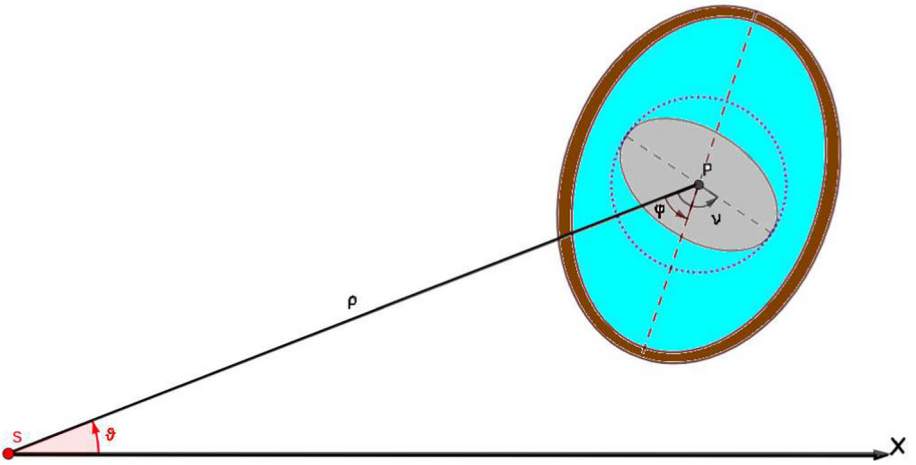

Fig. 1 Geometry of the system. Core (in gray) and crust (in brown) are separated by an ocean (in blue). The ocean is divided into two regions: an internal one attached to the core and an external one attached to the crust. The surface that separates the two regions is a sphere centered in P with radius equal to the semi-major axis of the core; it is represented by the dotted line

Let the central body be a massive point S fixed in the origin of reference frame and let P move on a Keplerian orbit around S. Let ρ be the distance PS, ϑ be the true anomaly and let φ and ν be the angles between the PS direction and direction of the major axis of the shell or the direction of the major axis of the core respectively. So, $\dot{\vartheta}$, $\dot{\varphi}$ and $\dot{\nu}$ are the orbital angular velocity and the angular velocities with respect to the central body of the shell and the core respectively.

To fix our notation and to increase the readability of the paper, we provide an independent derivation of the equation of motion of two-layer body already present in literature. In order to be able to insert friction in the system in terms of Rayleigh's dissipation function, we use a Lagrangian formalism.

The total kinetic energy is the sum of the kinetic energies of the two shells: the shell and the core.

$$\mathcal{T} = \frac{1}{2}m(\dot{\rho}^2 + \rho^2\dot{\vartheta}^2) + \frac{1}{2}C'(\dot{\varphi} + \dot{\vartheta})^2 + \frac{1}{2}C(\dot{\nu} + \dot{\vartheta})^2. \tag{1}$$

The potential energy is the sum of two pieces of gravitational attraction: the attraction between the core of the orbiting body and the central body and the attraction between the shell of the orbiting body and the central body:

$$\begin{aligned}\mathcal{V} &= -GM\int_V \frac{dm}{r} - GM\int_{V'} \frac{dm}{r} \\ &= -\frac{GM}{\rho}\left\{m + \frac{1}{4\rho^2}\left[A + B + 3(B - A)\cos(2\nu) + A' + B' + 3(B' - A')\cos(2\varphi)\right]\right\},\end{aligned} \tag{2}$$

where G is the universal gravitational constant, V the volume of the core and V' the volume of the shell.

So, the energy of the system is:

$$E = E_k + E_\varphi + E_\nu, \tag{3}$$

with

$$E_k = \frac{1}{2}m(\dot{\rho}^2 + \rho^2\dot{\vartheta}^2) - \frac{GMm}{\rho}, \tag{4}$$

$$E_\varphi = \frac{1}{2}C'(\dot{\varphi} + \dot{\vartheta})^2 - \frac{GM}{4\rho^3}\left[A' + B' + 3(B' - A')\cos(2\varphi)\right], \tag{5}$$

and

$$E_\nu = \frac{1}{2}C(\dot{\nu} + \dot{\vartheta})^2 - \frac{GM}{4\rho^3}\left[A + B + 3(B - A)\cos(2\nu)\right]. \tag{6}$$

We note that E_k is the well-known energy of the Kepler problem, that is constant on the Keplerian orbit, describing the motion of the center of mass of the orbiting body.

In what follows, we assume that the center of mass of the orbiting body moves unperturbed on its Keplerian trajectory.

On the other hand, E_φ and E_ν describe the dynamics associated with the shell and the core, respectively.

It is useful to consider the entire series of $(a/\rho)^3$ and ϑ in terms of eccentricity and mean anomaly, see Murray and Dermott (1999), namely:

$$\left(\frac{a}{\rho}\right)^3 = \sum_{n=0}^{\infty} a_n(e)e^n\cos(n\omega t), \tag{7}$$

with

$$a_n(e) = \sum_{l=0}^{\infty} b_{nl}e^{2l}, \tag{8}$$

and $b_{00} = 1$.

$$\vartheta = \omega t + \sum_{n=1}^{\infty} c_n(e)e^n\sin(n\omega t), \tag{9}$$

with

$$c_n(e) = \sum_{l=0}^{\infty} d_{nl}e^{2l}. \tag{10}$$

Hence,

$$\dot{\vartheta} = \omega + \sum_{n=1}^{\infty} n\omega c_n(e)e^n\cos(n\omega t). \tag{11}$$

So E_φ and E_ν can be written as (cfr. (7), (11)):

$$\begin{aligned} E_\varphi = {} & \frac{1}{2}C'\left(\dot{\varphi} + \omega + \sum_{n=1}^{\infty} n\omega c_n(e)e^n\cos(n\omega t)\right)^2 \\ & - \frac{\omega^2}{4}\left[A' + B' + 3(B' - A')\cos(2\varphi)\right]\sum_{n=0}^{\infty} a_n(e)e^n\cos(n\omega t) \end{aligned} \tag{12}$$

and

$$E_\nu = \frac{1}{2}C\left(\dot{\nu} + \omega + \sum_{n=1}^{\infty} n\omega c_n(e)e^n \cos(n\omega t)\right)^2 - \frac{\omega^2}{4}\left[A + B + 3(B - A)\cos(2\nu)\right]\sum_{n=0}^{\infty} a_n(e)e^n \cos(n\omega t), \tag{13}$$

where we have used the Kepler's third law: $\frac{GM}{a^3} = \omega^2$.

We can now consider a generic $2(k/2+1) : 2$ spin–orbit resonance, setting

$$\varphi = \frac{k\omega t}{2} + \gamma \quad \text{and} \quad \nu = \frac{k\omega t}{2} + \eta. \tag{14}$$

Indeed, according to our definition, the angle between the semi-major axis of the shell and the x-axis is $\vartheta + \varphi \simeq \omega t + \frac{k\omega t}{2} + \gamma = \left(\frac{k}{2}+1\right)\omega t + \gamma$; so the shell's angular speed with respect to the x-axis is $\left(\frac{k}{2}+1\right)\omega + \dot{\gamma}$, that is, the $2(k/2+1) : 2$ spin–orbit resonance condition, with γ the resonant angle. Same for the core.

Hence, (12) and (13) become:

$$E_\gamma = \frac{1}{2}C'\left[\left(\frac{k}{2}+1\right)\omega + \dot{\gamma} + \sum_{n=1}^{\infty} n\omega c_n(e)e^n \cos(n\omega t)\right]^2 - \frac{\omega^2}{4}\left[A' + B' + 3(B' - A')\cos(k\omega t + 2\gamma)\right]\sum_{n=0}^{\infty} a_n(e)e^n \cos(n\omega t) \tag{15}$$

and

$$E_\eta = \frac{1}{2}C\left[\left(\frac{k}{2}+1\right)\omega + \dot{\eta} + \sum_{n=1}^{\infty} n\omega c_n(e)e^n \cos(n\omega t)\right]^2 - \frac{\omega^2}{4}\left[A + B + 3(B' - A')\cos(k\omega t + 2\eta)\right]\sum_{n=0}^{\infty} a_n(e)e^n \cos(n\omega t). \tag{16}$$

Each of these expressions depend on two angles $\vartheta = \omega t$ and γ or η, respectively. According to our assumptions, ϑ is faster than γ and η (that vary very slowly); for this reason, we can consider the mean value of the energies E_γ and E_η over a period of ϑ.

$$\langle E_\gamma \rangle = \frac{1}{2}C'\left[\dot{\gamma}^2 + \left(\frac{k}{2}+1\right)^2\omega^2 + 2\left(\frac{k}{2}+1\right)\omega\dot{\gamma} + \sum_{n=1}^{\infty}\frac{n^2\omega^2 c_n^2(e)e^{2n}}{2}\right] - \frac{3}{8}\omega^2(B' - A')a_k(e)e^k\cos(2\gamma) \tag{17}$$

and

$$\langle E_\eta \rangle = \frac{1}{2}C\left[\dot{\eta}^2 + \left(\frac{k}{2}+1\right)^2\omega^2 + 2\left(\frac{k}{2}+1\right)\omega\dot{\eta} + \sum_{n=1}^{\infty}\frac{n^2\omega^2 c_n^2(e)e^{2n}}{2}\right] - \frac{3}{8}\omega^2(B - A)a_k(e)e^k\cos(2\eta). \tag{18}$$

The corresponding Lagrangian is:

$$\begin{aligned}\mathcal{L} = &\frac{1}{2}C'\left[\dot\gamma^2 + \left(\frac{k}{2}+1\right)^2\omega^2 + 2\left(\frac{k}{2}+1\right)\omega\dot\gamma + \sum_{n=1}^{\infty}\frac{n^2\omega^2c_n^2(e)e^{2n}}{2}\right]\\ &+\frac{3}{8}\omega^2(B'-A')a_k(e)e^k\cos(2\gamma)\\ &+\frac{1}{2}C\left[\dot\eta^2 + \left(\frac{k}{2}+1\right)^2\omega^2 + 2\left(\frac{k}{2}+1\right)\omega\dot\eta + \sum_{n=1}^{\infty}\frac{n^2\omega^2c_n^2(e)e^{2n}}{2}\right]\\ &+\frac{3}{8}\omega^2(B-A)a_k(e)e^k\cos(2\eta).\end{aligned} \tag{19}$$

The corresponding equations of motion are:

$$\begin{cases} C'\ddot\gamma = -\frac{3}{4}(B'-A')\omega^2a_k(e)e^k\sin 2\gamma\\ C\ddot\eta = -\frac{3}{4}(B-A)\omega^2a_k(e)e^k\sin 2\eta\end{cases} \tag{20}$$

that are the equations of two independent pendulums. These equations are well-known in literature, see, for instance equation (10) in Goldreich and Peale (1966) or equation (5.73) in Murray and Dermott (1999).[2]
So, for suitable initial conditions, $\gamma = 0$, $\eta = 0$ is a stable equilibrium point for the system. This implies that every $2(k/2+1) : 2$ spin–orbit resonance is stable.

3 Capture into spin–orbit resonance

In this section, we want to investigate the resonance capture mechanism. In order to do that we introduce in both the equations in (20) a coupled viscous friction (i.e., a friction proportional to the difference of velocity $\dot\varphi - \dot\nu = \dot\gamma - \dot\eta$). Moreover, in equation for η we introduce a second term of friction, proportional to $\dot\nu = \dot\eta + \frac{k\omega}{2}$ that gives the dissipation due to the non-perfect elasticity of the core.

A standard approach to treat a viscous friction in Lagrangian formalism is to use the Rayleigh's dissipation function R, defined as the function such that $\frac{\partial R}{\partial \dot q_i} = f_i$, where f_i is the frictional force acting on the i-th variable.
In our case, the Rayleigh's dissipation function assumes the form:

$$R = -\frac{1}{2}\lambda\,(\dot\varphi-\dot\nu)^2 - \frac{1}{2}\lambda'\dot\nu^2 = -\frac{1}{2}\lambda\,(\dot\gamma-\dot\eta)^2 - \frac{1}{2}\lambda'\left(\dot\eta+\frac{k\omega}{2}\right)^2, \tag{21}$$

with $\lambda > 0$ a viscous friction coefficient and $\lambda' \ll \lambda$ a viscoelastic friction coefficient.
The Euler–Lagrange equations become:

$$\begin{cases}\frac{\mathrm{d}}{\mathrm{d}t}\left(\frac{\partial\mathcal{L}}{\partial\dot\gamma}\right) = \frac{\partial\mathcal{L}}{\partial\gamma} + \frac{\partial R}{\partial\dot\gamma}\\ \frac{\mathrm{d}}{\mathrm{d}t}\left(\frac{\partial\mathcal{L}}{\partial\dot\eta}\right) = \frac{\partial\mathcal{L}}{\partial\eta} + \frac{\partial R}{\partial\dot\eta}\end{cases} \tag{22}$$

[2] Remark that we have the factor $\frac{3}{4}$ in Eq. (20) instead of the more familiar $\frac{3}{2}$. This is due to our choice of coordinates. Considering for instance the second equation in (14), our resonant angle differs from that defined in Murray and Dermott (1999), where using notation in Fig. 1 is $\theta + \nu - pM$. The difference between our resonant angle η and Murray & Dermott's one is $2e\sin M$, giving different factor in the averaged equation of motion.

Then, the equations of motion are:

$$\begin{cases} C'\ddot{\gamma} = -\frac{3}{4}(B'-A')\omega^2 a_k(e)e^k \sin 2\gamma - \lambda(\dot{\gamma}-\dot{\eta}) \\ C\ddot{\eta} = -\frac{3}{4}(B-A)\omega^2 a_k(e)e^k \sin 2\eta + \lambda(\dot{\gamma}-\dot{\eta}) - \lambda'(\dot{\eta}+\frac{k\omega}{2}) \end{cases} \tag{23}$$

As we already said, in principle in equation for γ, a friction term proportional to $\dot{\varphi} = \dot{\gamma} + \frac{k\omega}{2}$ must be present that gives the dissipation due to the non-perfect elasticity of the shell. Hence, equation of motion becomes:

$$\begin{cases} C'\ddot{\gamma} = -\frac{3}{4}(B'-A')\omega^2 a_k(e)e^k \sin 2\gamma - \lambda(\dot{\gamma}-\dot{\eta}) - \lambda''(\dot{\gamma}+\frac{k\omega}{2}) \\ C\ddot{\eta} = -\frac{3}{4}(B-A)\omega^2 a_k(e)e^k \sin 2\eta + \lambda(\dot{\gamma}-\dot{\eta}) - \lambda'(\dot{\eta}+\frac{k\omega}{2}), \end{cases} \tag{24}$$

but since it is reasonable assume that the shell is much lighter than the core, then $\lambda'' << \lambda'$. For this reason, we will neglect this term that, in any case, does not add anything to the general description.[3]

Equation (23) can be rewritten in terms of first-order ones:

$$\begin{cases} C'\dot{v_\gamma} = -\frac{3}{4}(B'-A')\omega^2 a_k(e)e^k \sin 2\gamma - \lambda(v_\gamma - v_\eta) \\ \dot{\gamma} = v_\gamma \\ C\dot{v_\eta} = -\frac{3}{4}(B-A)\omega^2 a_k(e)e^k \sin 2\eta + \lambda(v_\gamma - v_\eta) - \lambda'(v_\eta + \frac{k\omega}{2}) \\ \dot{\eta} = v_\eta \end{cases} \tag{25}$$

In Sect. 5, we solve numerically this system of nonlinear coupled differential equations for different values of initial conditions.

Nevertheless, here we want to study analytically the behavior of the system. In order to do that we note that v_γ varies with a characteristic time $\tau_\gamma = \frac{C'}{\lambda}$, while v_η varies with a characteristic time $\tau_\eta = \frac{C}{\lambda}$. Hence, if $C' \ll C$ then $\tau_\eta \gg \tau_\gamma$[4]; in this case, v_η varies very slowly compared to v_γ, and then we can study the evolution of v_γ in (25) considering v_η as a constant. This is equivalent to decoupling the four equations in (25) into two velocity fields $\mathbf{f}_\gamma$ and $\mathbf{f}_\eta$.

Let us consider then $\mathbf{f}_\gamma$, with v_η constant:

$$\begin{cases} C'\dot{v_\gamma} = -\frac{3}{4}(B'-A')\omega^2 a_k(e)e^k \sin 2\gamma - \lambda v_\gamma + \lambda v_\eta \\ \dot{\gamma} = v_\gamma \end{cases} \tag{26}$$

The equilibrium points are of the form $(\bar{\gamma}; 0)$ and $(\frac{\pi}{2} - \bar{\gamma}; 0)$, with $\bar{\gamma} = \frac{1}{2}\arcsin\left(\frac{4\lambda v_\eta}{3(B'-A')\omega^2 a_k(e)e^k}\right)$.

These equilibrium point exist if and only if

$$\frac{4\lambda|v_\eta|}{3(B'-A')\omega^2 a_k(e)e^k} < 1 \implies |v_\eta| < \frac{3(B'-A')\omega^2 a_k(e)e^k}{4\lambda}, \tag{27}$$

namely if the core is rotating with a velocity not too far from the resonance one.

The physical meaning is straightforward. If the friction term λv_η is bigger than the torque, then the shell stays glued to the core and the two rotate together. If the condition (27) is not satisfied, then the solution of the equations, after a small transient, is characterized by a γ that grows linearly in time and a v_γ that oscillates very slowly around the value v_η: $\langle\dot{\varphi}\rangle = \langle\dot{v}\rangle$.

[3] For an explicit expression of λ' or λ'' see Eq. (48) below.

[4] See below for numerical estimates.

On the other side, if the condition (27) is satisfied, then the friction term is weaker than the torque and in this case gravitational attraction of the central body brings the shell into the spin–orbit resonance (that is the equilibrium point).

Notice that in our model, the shell will certainly (with probability 1) reach the equilibrium point if the condition (27) is satisfied, which will certainly be verified after a long enough time since v_η is slowly decreasing due to the presence of friction terms.

Once the shell reaches the resonance, slowly it brings the core into the resonance as well. Indeed, if the shell is in resonance, then $v_\gamma = 0$, so $\mathbf{f}_\eta$ in (25) become:

$$\begin{cases} C\dot{v_\eta} = -\frac{3}{4}(B-A)\omega^2 a_k(e)e^k \sin 2\eta - (\lambda+\lambda')v_\eta - \lambda'\frac{k\omega}{2} \\ \dot{\eta} = v_\eta \end{cases} \tag{28}$$

In order to simplify the notation, we can rescale the first equation, obtaining:

$$\begin{cases} \dot{v_\eta} = -\frac{1}{2}\varepsilon\omega^2 a_k(e)e^k \sin 2\eta - \frac{(\lambda+\lambda')}{C}v_\eta - \frac{\lambda'}{C}\frac{k\omega}{2} \\ \dot{\eta} = v_\eta, \end{cases} \tag{29}$$

with $\varepsilon = \frac{3}{2}\frac{(B-A)}{C}$.

The equilibrium points are of the form $(\bar{\eta}; 0)$ and $(\frac{\pi}{2} - \bar{\eta}; 0)$, with $\bar{\eta} = \frac{1}{2}\arcsin\left(\frac{k\lambda'/C}{\varepsilon\omega a_k(e)e^k}\right)$.

These equilibrium points exist if and only if

$$\frac{k\lambda'/C}{\varepsilon\omega a_k(e)e^k} < 1 \implies e^k > \frac{k\lambda'}{\varepsilon C\omega a_k(e)}, \tag{30}$$

namely if the eccentricity is big enough.

The equilibrium point $(\bar{\eta}; 0)$ is asymptotically stable if it exists a Lyapunov function $W(\eta, v_\eta)$ such that W has a minimum in $(\bar{\eta}, 0)$ and $\nabla\mathbf{W}\cdot\mathbf{f}_\eta \le 0$.

A Lyapunov function is:

$$W(\eta, v_\eta) = \frac{1}{2}v_\eta^2 - \frac{1}{4}\varepsilon\omega^2 a_k(e)e^k \cos 2\eta + \frac{\lambda'}{C}\frac{k\omega}{2}\eta. \tag{31}$$

Indeed

$$\begin{aligned} \nabla\mathbf{W}\cdot\mathbf{f}_\eta &= \frac{\partial W}{\partial v_\eta}\cdot\dot{v_\eta} + \frac{\partial W}{\partial\eta}\cdot\dot{\eta} \\ &= v_\eta\left[-\frac{1}{2}\varepsilon\omega^2 a_k(e)e^k \sin 2\eta - \frac{(\lambda+\lambda')}{C}v_\eta - \frac{\lambda'}{C}\frac{k\omega}{2}\right] \\ &\quad + \left[\frac{1}{2}\varepsilon\omega^2 a_k(e)e^k \sin 2\eta + \frac{\lambda'}{C}\frac{k\omega}{2}\right]v_\eta = -\frac{(\lambda+\lambda')}{C}v_\eta^2 \le 0. \end{aligned} \tag{32}$$

So we can consider the Lyapunov function as an effective energy:

$$E_{\text{eff}} = \frac{1}{2}\dot{\eta}^2 + V_{\text{eff}} \tag{33}$$

such that

$$\frac{\mathrm{d}E_{\text{eff}}}{\mathrm{d}t} = -\frac{(\lambda+\lambda')}{C}\dot{\eta}^2 \tag{34}$$

and

$$V_{\text{eff}} = -\frac{1}{2}\varepsilon\omega^2 a_k(e)e^k \cos 2\eta + \frac{\lambda'}{C}\frac{k\omega}{2}\eta. \tag{35}$$

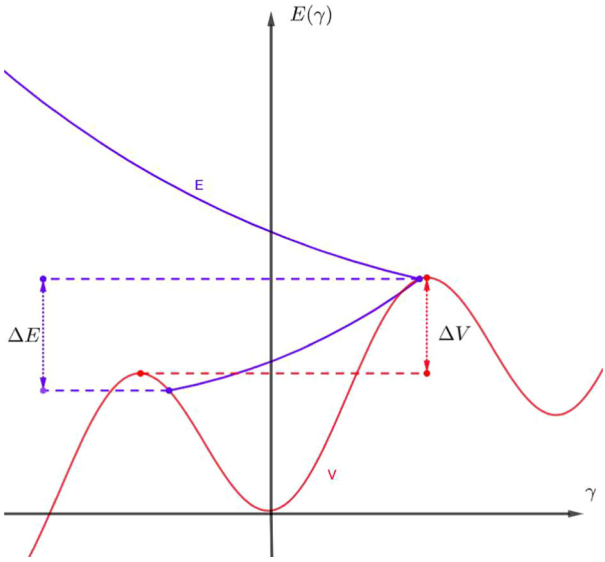

Fig. 2 Graphical representation of the condition that ensure the capture in resonance: the energy dissipation $|\Delta E_{\rm eff}|$ between two maxima of the potential is bigger than the corresponding potential variation $|\Delta V_{\rm eff}|$. The scale on the y-axis has been voluntarily increased

Now, following the already mentioned pioneering papers (Goldreich and Peale 1966, 1967), we can find a condition which ensure that the equilibrium point is reached. Indeed the core will certainly (with probability 1) reach the resonance if the energy dissipation $|\Delta E_{\rm eff}|$ between two maxima of the potential (e.g., between $-\frac{\pi}{2}$ and $\frac{\pi}{2}$) is bigger than the corresponding potential variation $|\Delta V_{\rm eff}|$.

$|\Delta V_{\rm eff}|$ is easy to determine:

$$|\Delta V_{\rm eff}| = \left|V_{\rm eff}\left(\frac{\pi}{2}\right) - V_{\rm eff}\left(-\frac{\pi}{2}\right)\right| = \frac{\lambda'}{C}\frac{k\omega}{2}\pi. \tag{36}$$

While $|\Delta E_{\rm eff}|$ can be determine integrating $\frac{{\rm d}E_{\rm eff}}{{\rm d}\eta}$ from $-\frac{\pi}{2}$ to $\frac{\pi}{2}$:

$$\begin{aligned} |\Delta E_{\rm eff}| &= \left|\int_{-\frac{\pi}{2}}^{\frac{\pi}{2}}\left(\frac{{\rm d}E_{\rm eff}}{{\rm d}\eta}\right){\rm d}\eta\right| = \left|\int_{-\frac{\pi}{2}}^{\frac{\pi}{2}}\frac{(\lambda+\lambda')}{C}\dot{\eta}{\rm d}\eta\right| \\ &= \frac{(\lambda+\lambda')}{C}\int_{-\frac{\pi}{2}}^{\frac{\pi}{2}}\sqrt{2(E_{\rm eff}-V_{\rm eff})}{\rm d}\eta \end{aligned} \tag{37}$$

To solve the integral, we can replace $V_{\rm eff}$ with $V > V_{\rm eff}$, obtaining a lower bound for $|\Delta E_{\rm eff}|$. Moreover, as we can see in Fig. 2, we can imagine that the motion reverses its direction near to the maximum of the potential (in this way we still get a lower bound):

$$\begin{aligned} |\Delta E_{\rm eff}| &\geq \frac{(\lambda+\lambda')}{C}\int_{-\frac{\pi}{2}}^{\frac{\pi}{2}}\sqrt{2(E_{\rm eff}-V)}{\rm d}\eta \\ &\geq \frac{(\lambda+\lambda')}{C}\int_{-\frac{\pi}{2}}^{\frac{\pi}{2}}\sqrt{2\frac{1}{2}\varepsilon\omega^2 a_k(e)e^k(1+\cos 2\eta)}{\rm d}\eta \\ &= \frac{(\lambda+\lambda')}{C}\omega\sqrt{\varepsilon a_k(e)e^k}\int_{-\frac{\pi}{2}}^{\frac{\pi}{2}}\sqrt{1+\cos 2\eta}{\rm d}\eta = \frac{(\lambda+\lambda')}{C}\omega\sqrt{8\varepsilon a_k(e)e^k} \end{aligned} \tag{38}$$

where we have used the relation $1+\cos 2\eta = 2\cos^2\eta$.

So, the core will reach the $2(k/2+1):2$ spin–orbit resonance with probability 1 if:

$$|\Delta E_{\rm eff}| > |\Delta V_{\rm eff}| \implies \frac{(\lambda+\lambda')}{C}\omega\sqrt{8\varepsilon a_k(e)e^k} > \frac{\lambda'}{C}\frac{k\omega}{2}\pi \implies \frac{\lambda}{\lambda'} > \frac{k\pi}{\sqrt{32\varepsilon a_k(e)e^k}} - 1, \tag{39}$$

namely if λ is sufficiently larger than λ'.

An analogous computation for the capture in resonance of the shell has been omitted because the linear term in its Lyapunov function has the opposite sign, implying the capture with probability 1.

Notice that in the pioneering works (Goldreich and Peale 1966, 1967), no assumptions are made about the internal structure of the orbiting body, so in that model the additional viscous dissipation is absent, while it is a fundamental ingredient in our model. We can therefore think that our model generalizes that of Goldreich and Peale, indeed setting $\lambda = 0$ (i.e., neglecting the viscous friction between the two layers) our equation of motion for η in (23) becomes the equation (10) with torque (12a) in Goldreich and Peale (1966); therefore, in this case, the problem of a small capture probability arises. On the contrary, if one consider, like we did, also the internal viscous dissipation between the layers of the orbiting body, that problem is overcome: the core is certainly (with probability 1) captured into the resonance if conditions (30) and (39) are satisfied, namely, respectively, it the eccentricity is big enough and if the viscous dissipation is bigger enough with respect the viscoelastic one.[5]

4 Exit from the resonance

When the core and the shell are both in resonance, they rotate together with the same angular speed: $\dot\varphi = \dot\upsilon = \frac{k\omega}{2} \implies v_\gamma = v_\eta = 0$, so the viscous dissipation in both the equations for γ and η vanishes.

In such a situation the only dissipation source is the viscoelastic term $\lambda'\frac{k\omega}{2}$:

$$\begin{cases} C'\dot{v_\gamma} = -\frac{3}{4}(B'-A')\omega^2 a_k(e)e^k \sin 2\gamma \\ \dot\gamma = v_\gamma \\ C\dot{v_\eta} = -\frac{3}{4}(B-A)\omega^2 a_k(e)e^k \sin 2\eta - \lambda'\frac{k\omega}{2} \\ \dot\eta = v_\eta \end{cases} \tag{40}$$

Although the dissipation $\lambda'\frac{k\omega}{2}$ is very small, it slowly tends to circularize the orbit.
When the eccentricity becomes so small that condition (30) is no longer satisfied, then the system exit from the $2(k/2+1):2$ and, while the shell and the core still rotate at the same angular speed, it further decreases until the system reaches, with the same mechanisms, the $2(k'/2+1):2$ spin–orbit resonance, with $k' = k-1$.
The second to last resonance that the system visits is the $3:2$ spin–orbit resonance($k=1$), as in Sun-Mercury system. The last is, of course, the $1:1$ spin orbit resonance ($k=0$), as in Jupiter-Ganymede system.

[5] See below for numerical estimates.

5 Numerical simulations

In this section, we present some preliminary numerical simulations integrating the set of coupled Eq. (25) using Mathematica.

The purpose of these simulations is to qualitatively observe the dynamics of the system and to note the presence of different time scales in order to justify the assumptions made before regarding the way to decouple the equations.

More in-depth simulations will be the subject of future works, as well as simulations regarding the orbital dynamics of systems in $1:1$ spin–orbit resonance. The aim is to observe how the internal structure modeled in this paper can influence the evolution of systems in $1:1$ spin orbit resonance, such as the Jupiter-Ganymede system. This could provide a support framework for the JUICE mission to analyze the data collected by the space craft.

In order to perform the numerical integration in a more handy way, we rewrite Eq. (25) as:

$$\begin{cases} \dot{v_\gamma} = -\frac{1}{2}\varepsilon'\omega^2 a_k(e)e^k \sin 2\gamma - \frac{1}{\tau_\gamma}(v_\gamma - v_\eta) \\ \dot{\gamma} = v_\gamma \\ \dot{v_\eta} = -\frac{1}{2}\varepsilon\omega^2 a_k(e)e^k \sin 2\eta + \frac{1}{\tau_\eta}(v_\gamma - v_\eta) - \frac{1}{\tau'_\eta}(v_\eta + \frac{k\omega}{2}) \\ \dot{\eta} = v_\eta \end{cases} \tag{41}$$

with $\tau_\gamma = \frac{C'}{\lambda}$, $\tau_\eta = \frac{C}{\lambda}$ and $\tau'_\eta = \frac{C}{\lambda'}$.

For the purpose of this work, we focus our simulations on a particular spin orbit resonance, namely the 3:2. This correspond to set $k = 1$ and consequently $a_k(e)$ evaluated at $e = 0$ is $a_1(0) = 3$; the exploration of the cascade in subsequent spin orbit resonances will be the subject of future works.

Finally, in order to obtain plausible simulations, we consider the parameters values of Ganymede, summarized in Table 1.

The equations become the following:

$$\begin{cases} \dot{v_\gamma} = -0,02 \sin 2\gamma - 0.03(v_\gamma - v_\eta) \\ \dot{\gamma} = v_\gamma \\ \dot{v_\eta} = -0,02 \sin 2\eta + 3 \times 10^{-5}(v_\gamma - v_\eta) - 3 \times 10^{-8}(v_\eta + 150) \\ \dot{\eta} = v_\eta \end{cases} \tag{42}$$

where we have expressed the coefficients until the first significant digit, and we have used S.I. units except for time, which is expressed in years.[6]

We first integrated the equations for 10^5 iterations with initial conditions $(\gamma; v_\gamma; \eta; v_\eta) = \left(0.1; 1000\,\frac{1}{y}; 0.1; 50\,\frac{1}{y}\right)$, i.e., when v_η does not satisfy condition (27); the result are shown in Fig. 3. As we can see, in this case v_γ decreases on a very short time until it reaches the value of v_η and from then it oscillates around this value (left picture in Fig. 3) never approaching zero. v_η, on the contrary, remains almost constant; indeed it decreases very slowly on a very long time scale (right picture in Fig. 3). The physical meaning is straightforward; v_η is large enough that the friction term is bigger than the gravitational torque, then the shell stays glued to the core and the two rotate together.

Then, we integrated the equations for 10^7 iterations with initial conditions $(\gamma; v_\gamma; \eta; v_\eta) = \left(0.1; 1000\,\frac{1}{y}; 0.1; 5\,\frac{1}{y}\right)$, i.e., when v_η satisfies condition (27); the result are shown in Fig. 4.

[6] For an estimate of the parameters see Eq. (52) below.

Table 1 Physical parameter values expressed with two significant digits in SI units

Table of physical parameter values	Ganymede	Mercury
Mean motion (ω)	1.0×10^{-5}	8.3×10^{-7}
Semi-major axis (a)	1.1×10^{9}	5.8×10^{10}
Eccentricity (e)	1.3×10^{-3}	2.1×10^{-1}
Mean radius (R)	2.6×10^{6}	2.4×10^{6}
Mass (m)	1.5×10^{23}	3.3×10^{23}
Equatorial ellipticity (ε)	(10^{-3})	(6×10^{-5})
Tidal quality factor (Q)	(100)	(100)
Tidal Love number (K_2)	(0.02)	(0.1)
Viscosity of ocean/mantle ($\bar{\eta}$)	(1.6×10^{-3})	(10^{3})
Thickness of ocean/mantle (h)	(10^{5})	(4×10^{5})

The values without brackets are taken from NASA Fact Sheet
The values of ε are computed using data in Zubarev et al. (2015) and Karimi et al. (2016) respectively
The values of Q and K_2 of Mercury are taken from Murray and Dermott (1999)
For Ganymede, we use the same values of Q and K_2 of Europa, taken from Murray and Dermott (1999); indeed it seems reasonable to think that the internal structure of the two satellites; therefore, the tidal response, is similar. These values are just a numerical estimates, indeed neither Ganymede's nor Europa's K_2/Q are known for sure. One of the tasks of JUICE mission is to estimate these parameters
The values of $\bar{\eta}$ of Ganymede and Mercury are that of water and magma, respectively
The values of h of Ganymede and Mercury are taken from Hay and Matsuyama (2019) and Hauck et al. (2013), respectively

As we can see, in this case, v_γ vanishes on a very short time and from then it oscillates around zero (left picture in Fig. 4). v_η, on the contrary, also vanishes but on a longer time scale (right picture in Fig. 4). The physical meaning is straightforward: v_η is small enough that the friction term is lesser than the gravitational torque, then the latter brings the shell into the spin–orbit resonance and, slowly, the core enter the resonance too.

At some point the system will exit from resonance. This process occurs in a very long time scales.[7] In this paper, we are not interested in the numerical investigation of this process that will be the subject of future works.

6 Astronomical estimates

In this section, we want to propose a possible way to estimate some quantities involved in our model from values know in the literature, summarized in Table 1.

To this end, let us consider the equation for v_η in (25):

$$C\dot{v_\eta} = -\frac{3}{4}(B-A)\omega^2 a_k(e)e^k \sin 2\eta + \lambda(v_\gamma - v_\eta) - \lambda'\left(v_\eta + \frac{k\omega}{2}\right)$$

[7] See below for numerical estimates.

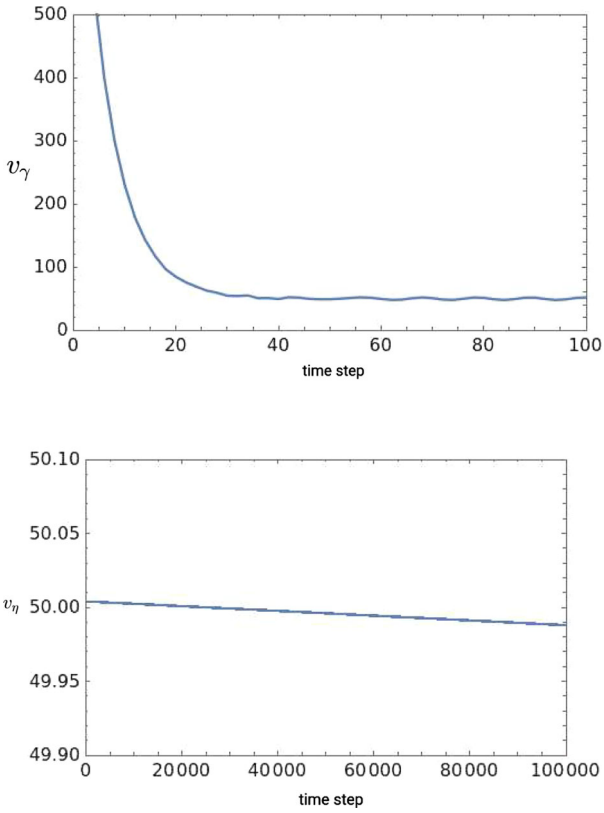

Fig. 3 Numerical solution for the system with initial conditions $(\gamma; v_\gamma; \eta; v_\eta) = \left(0.1; 1000\,\frac{1}{y}; 0.1; 50\,\frac{1}{y}\right)$, i.e., when v_η does not satisfy condition (27). In the picture on the left, we have plotted v_γ versus time for 100 time steps. As we can see, after about 30 time steps, v_γ reaches the value of v_η and oscillates around it. In the picture on the right, we have plotted v_η versus time for 100000 time steps. As we can see, v_η remains almost constant: indeed it decreases very slowly on a very long time scale

$$= -\frac{3}{4}(B-A)\omega^2 a_k(e)e^k \sin 2\eta + T_v + T_t, \tag{43}$$

with $T_v = \lambda(v_\gamma - v_\eta)$ the viscous torque and $T_t = -\lambda'(v_\eta + \frac{k\omega}{2})$ the viscoelastic tidal torque.

We can compute T_v considering a two-layer body having a solid core that rotates with angular speed v_v and a solid crust that rotates with angular speed v_φ, separated by a fluid (i.e., an ocean) of thickness h. Hence, the crust rotates with velocity $v_{\rm rel} = v_v - v_\varphi = v_\eta - v_\gamma$ with respect to the core. In a point at distance r from the rotational axis, the tangential relative velocity is: $v_{\rm rel}\, r$.

Finally, let us suppose that the viscous friction force per unit surface is $\bar\eta$ times the gradient of tangential relative velocity, or, if you prefer, by definition of viscosity ($\bar\eta$): $F_v = \bar\eta\, v_{\rm rel}\, r/h$. Hence, the friction torque with respect the rotational axis acting on the core is obtained by integrating over all the core's surface Σ_c:

$$|T_v| = \int_{\Sigma_c} F_v\, r\, {\rm d}\sigma = \int_0^{2\pi}\int_0^{\pi} \frac{\bar\eta(v_\eta - v_\gamma)r}{h} r R^2 \sin\vartheta {\rm d}\vartheta {\rm d}\phi, \tag{44}$$

with $r = R\sin\vartheta$ the distance between the rotational axis (z-axis) and the point of geographic coordinate (ϕ, ϑ).

$$|T_v| = 2\pi \frac{\bar\eta(v_\eta - v_\gamma)R^4}{h}\int_0^{\pi} \sin^3\vartheta {\rm d}\vartheta = \frac{8\pi}{3}\frac{\bar\eta(v_\eta - v_\gamma)R^4}{h}. \tag{45}$$

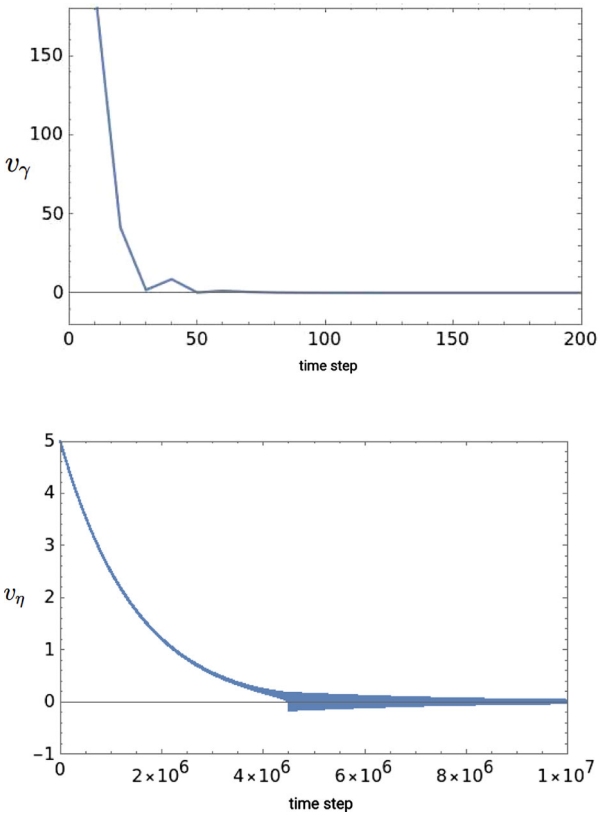

Fig. 4 Numerical solution for the system with initial conditions $(\gamma; v_\gamma; \eta; v_\eta) = \left(0.1; 1000\,\frac{1}{y}; 0.1; 5\,\frac{1}{y}\right)$, i.e., when v_η satisfies condition (27). In the picture on the left, we have plotted v_γ versus time for 200 time steps. As we can see, after about 50 time steps, v_γ vanishes and oscillates around zero. In the picture on the right, we have plotted v_η versus time for 10^7 time steps. As we can see, v_η vanishes but on a much longer time scale (on the order of 10^6 iterations)

So, the friction coefficient λ used from (23) onward is given by:

$$\lambda = \frac{8\pi}{3}\frac{\bar{\eta}R^4}{h}. \tag{46}$$

Note that this expression of λ represents a lower bound. Indeed, our assumption on a laminar flow is a convenient way to find an explicit expression of λ. Some recent papers predict non-laminar flow in the subsurface oceans of icy satellites, see for instance (Hay and Matsuyama 2019), where the effects of turbulent subsurface oceans are numerically modeled. Moreover, as we already said, others kinds of couplings between core and shell are treated in literature. In Correia and Laskar (2009) and Williams et al. (2001), an expression of the effective friction coefficient due to both viscous and electromagnetic coupling is given. In any case, considering turbulent regimes or considering other sources of dissipation, the value of λ will be greater than the one we found and condition (39) is even more satisfied.

The estimate of λ' can be found considering the expression of T_t given by the MacDonald's tidal torque formula (equation 4.159 in Murray and Dermott (1999)):

$$|T_t| = \frac{3}{2}\frac{k_2}{Q}\frac{Gm^2R^5}{a^6}. \tag{47}$$

Hence, if we suppose $v_\eta < \omega$:

$$\lambda' = \frac{3}{k\omega}\frac{k_2}{Q}\frac{Gm^2R^5}{a^6}. \tag{48}$$

Finally,

$$\frac{\lambda}{\lambda'} = \frac{8\pi\bar{\eta}a^6Qk\omega}{9hk_2Gm^2R} \tag{49}$$

Considering the values of the parameters known in the literature (Table 1), we obtain the estimate of λ/λ' for Ganymede and Mercury is:

$$\left(\frac{\lambda}{\lambda'}\right)_G \simeq 10^3; \qquad \left(\frac{\lambda}{\lambda'}\right)_M \simeq 10^{16}. \tag{50}$$

If we now consider condition (39) for $k = 1$ (3 : 2 spin–orbit resonance), we can see that for Mercury's parameters, it is certainly satisfied. Whereas in the case of Ganymede, the condition require an λ/λ' ratio exactly of the same order as the one we estimate using current values for the parameters, so is not obvious that Ganymede could have trapped into the 3 : 2 spin–orbit resonance or even if it has been trapped in the past, its present small eccentricity is probably not compatible with the 3 : 2 spin–orbit resonance. Since some of Ganymede's parameters are not known exactly, but in a range, the values of λ/λ' ratio could be update in future with more accurate measurements.

Finally, the estimate value $\left(\frac{\lambda}{\lambda'}\right)_M \simeq 10^{16}$ is a purely indicative lower bound; indeed in the case of Mercury, we expect that λ' is bigger than the value we found since the molten mantle too gives an important contribution to the dissipation. Nevertheless, an in-depth study of this aspect is beyond the aim of this work.

7 Characteristic time scales

In this section, we want to estimate the characteristic time scales of the system in order to justify all the assumptions we made regarding the decoupling of Eq. (25):

$$\begin{cases} C'\dot{v_\gamma} = -\frac{3}{4}(B'-A')\omega^2 a_k(e)e^k \sin 2\gamma - \lambda(v_\gamma - v_\eta) \\ \dot{\gamma} = v_\gamma \\ C\dot{v_\eta} = -\frac{3}{4}(B-A)\omega^2 a_k(e)e^k \sin 2\eta + \lambda(v_\gamma - v_\eta) - \lambda'(v_\eta + \frac{k\omega}{2}) \\ \dot{\eta} = v_\eta \end{cases} \tag{51}$$

As we have seen in the paper, we can identify three well-separated processes: the entrance in resonance for the shell, the entrance in resonance for the core and the exit from resonance.

We will see that these three processes occur on very different time scales. Indeed, the entrance in resonance for the shell occurs in a characteristic time $\tau_\gamma = \frac{C'}{\lambda}$ (characteristic time of the dynamics of v_γ).

On the other hand, the entrance in resonance for the core occurs in a characteristic time $\tau_\eta = \frac{C}{\lambda}$ (characteristic time of the dynamics of v_η).

Finally, the exit from resonance occurs in a characteristic time $\tau'_\eta = \frac{C}{\lambda'}$ (characteristic time of the dynamics of v_η in Eq. (40) that coincides with the characteristic time of the dynamics of the eccentricity).

Since $C' \ll C$ and $\lambda' \ll \lambda$, then $\tau_\gamma << \tau_\eta << \tau'_\eta$ and thus the three processes mentioned above have a well-separated time scales.

Since $C \propto R^5$, it is reasonable to assume that C'/C of the order 10^{-3} or 10^{-4}; indeed the thickness of the shell is about $10^4\, m$ or $10^5\, m$ while the radius of the core is about $10^6\, m$ for both Mercury and Ganymede.

The estimate of τ_γ; τ_η; τ'_η for Ganymede are:

$$\tau_\gamma \simeq 10^9\, s; \qquad \tau_\eta \simeq 10^{12}\, s; \qquad \tau'_\eta \simeq 10^{15}\, s. \tag{52}$$

We note that τ'_η, that is the characteristic time of exit from resonance, coincides with the characteristic time of variation of eccentricity. Our value is in good agreement with that known in literature:
$10^8\, y \simeq 10^{15}\, s$, see, for instance (Murray and Dermott 1999; Showman et al. 1997).

8 Conclusions

In our model, we assume that the body is composed by an inner solid core and an outer solid crust separated by a viscous liquid layer (ocean or mantle). We derive the following mechanism to enters an arbitrary spin–orbit resonance. The (much lighter) crust usually rotates jointly with the core. A viscoelastic tidal torque acting on the core is always present that slowly decreases the angular velocity of the whole body. When the angular velocity of such whole body becomes sufficiently close to a resonance (condition (27)), the crust is certainly captured in resonance on a very small time scale. Then, if the contribution of the viscoelastic friction is sufficiently small with respect to the viscous coupling between crust and core (condition (39)), the core is driven, again with certainty, to the same resonance on a different and slightly longer time scale. The body, then, exits from resonance when the action of the viscoelastic torque reduces the eccentricity of the orbit under a certain limit value (condition (30)), and this happens on a third longer time scale. The whole process causes a cascade of spin–orbit resonances, bringing eventually the system in the stable 1:1 state.

The implication of our model on the dynamics of a body in $1:1$ spin orbit resonance with its central body will be the subject of future works.

Acknowledgements The authors want to thank the anonymous referees whose contribution helped to improve the readability of the paper. We benefited of several comments by Christoph Lhotka and Giuseppe Pucacco. BS acknowledges the support of the Italian MIUR Department of Excellence Grant (CUP E83C18000100006). MV has been supported through the ASI Contract n.2023-6-HH.0, Scientific Activities for JUICE, E phase (CUP F83C23000070005).

Author Contributions All the authors contributed equally to this work.

Funding Open access funding provided by Università degli Studi di Roma Tor Vergata within the CRUI-CARE Agreement.

Data Availability No datasets were generated or analyzed during the current study.

Declarations

Conflict of interest The authors declare no conflict of interest.

References

Antognini, F., Biasco, L., Chierchia, L.: The spin–orbit resonances of the solar system: a mathematical treatment matching physical data. J. Nonlinear Sci. **24**, 473–492 (2014)

Apollonio, V., D'Autilia, R., Scoppola, B., Scoppola, E., Troiani, A.: Criticality of measures on 2-d Ising configurations: from square to hexagonal graphs. J. Stat. Phys. **177**(5), 1009–1021 (2019)

Apollonio, V., D'Autilia, R., Scoppola, B., Scoppola, E., Troiani, A.: Shaken dynamics: an easy way to parallel Markov chain Monte Carlo. J. Stat. Phys. **189**(3), 39 (2022a)

Apollonio, V., Jacquier, V., Nardi, F.R., Troiani, A.: Metastability for the Ising model on the hexagonal lattice. Electron. J. Probab. **27**, 1–48 (2022b)

Baland, R.-M., Yseboodt, M., Van Hoolst, T.: Obliquity of the Galilean satellites: the influence of a global internal liquid layer. Icarus **220**(2), 435–448 (2012)

Baland, R.-M., Coyette, A., Van Hoolst, T.: Coupling between the spin precession and polar motion of a synchronously rotating satellite: application to titan. Celest. Mech. Dyn. Astron. **131**, 1–50 (2019)

Bartuccelli, M.V., Deane, J.H., Gentile, G.: The high-order Euler method and the spin–orbit model. A fast algorithm for solving differential equations with small, smooth nonlinearity. Celest. Mech. Dyn. Astron. **121**, 233–260 (2015)

Calleja, R., Celletti, A., Gimeno, J., Llave, R.: Kam quasi-periodic tori for the dissipative spin–orbit problem. Commun. Nonlinear Sci. Numer. Simul. **106**, 106099 (2022)

Cappuccio, P., Hickey, A., Durante, D., Di Benedetto, M., Iess, L., De Marchi, F., Plainaki, C., Milillo, A., Mura, A.: Ganymede's gravity, tides and rotational state from JUICE's 3GM experiment simulation. Planet. Space Sci. **187**, 104902 (2020)

Celletti, A., Chierchia, L.: Hamiltonian stability of spin–orbit resonances in celestial mechanics. Celest. Mech. Dyn. Astron. **76**, 229–240 (2000)

Chen, Q., Pinzari, G.: Exponential stability of fast driven systems, with an application to celestial mechanics. Nonlinear Anal. **208**, 112306 (2021)

Corbi, F., Funiciello, Faccenna, C., Ranalli, G., Heuret, A.: Seismic variability of subduction thrust faults: insights from laboratory models. J. Geophys. Res. **116**, 1–14 (2011)

Correia, A.C., Laskar, J.: Mercury's capture into the 3/2 spin–orbit resonance including the effect of core-mantle friction. Icarus **201**(1), 1–11 (2009)

Correia, A.C., Laskar, J.: Long-term evolution of the spin of mercury: I. Effect of the obliquity and core-mantle friction. Icarus **205**(2), 338–355 (2010)

Correia, A., Ragazzo, C., Ruiz, L.: The effects of deformation inertia (kinetic energy) in the orbital and spin evolution of close-in bodies. Celest. Mech. Dyn. Astron. **130**, 1–30 (2018)

Coyette, A., Van Hoolst, T., Baland, R.-M., Tokano, T.: Modeling the polar motion of titan. Icarus **265**, 1–28 (2016)

D'Autilia, R., Andrianaivo, L.N., Troiani, A.: Parallel simulation of two-dimensional Ising models using probabilistic cellular automata. J. Stat. Phys. **184**, 1–22 (2021)

Efroimsky, M.: Tidal evolution of asteroidal binaries. Ruled by viscosity. Ignorant of rigidity. Astron. J. **150**(4), 98 (2015)

Efroimsky, M., Makarov, V.V.: Tidal friction and tidal lagging. Applicability limitations of a popular formula for the tidal torque. Astrophys. J. **764**(1), 26 (2013)

Ferraz-Mello, S., Grotta-Ragazzo, C., Santos, L.R.: Dissipative forces in celestial mechanics. 30o colóquio brasileiro de matemática. Publicaçoes Matemáticas, IMPA (2015)

Folonier, H.A., Ferraz-Mello, S.: Tidal synchronization of an anelastic multi-layered body: Titan's synchronous rotation. Celest. Mech. Dyn. Astron. **129**, 359–396 (2017)

Goldreich, P., Peale, S.: Spin-orbit coupling in the solar system. Astron. J. **71**, 425 (1966)

Goldreich, P., Peale, S.: Spin-orbit coupling in the solar system. II. The resonant rotation of Venus. Astron. J. **72**, 662 (1967)

Gomez Casajus, L., Ermakov, A., Zannoni, M., Keane, J., Stevenson, D., Buccino, D., Durante, D., Parisi, M., Park, R., Tortora, P., et al.: Gravity field of Ganymede after the Juno extended mission. Geophys. Res. Lett. **49**(24), 2022–099475 (2022)

Hauck, S.A., Margot, J.-L., Solomon, S.C., Phillips, R.J., Johnson, C.L., Lemoine, F.G., Mazarico, E., McCoy, T.J., Padovan, S., Peale, S.J., et al.: The curious case of mercury's internal structure. J. Geophys. Res. Planets **118**(6), 1204–1220 (2013)
Hay, H.C., Matsuyama, I.: Nonlinear tidal dissipation in the subsurface oceans of Enceladus and other icy satellites. Icarus **319**, 68–85 (2019)
Karimi, R., Ardalan, A.A., Farahani, S.V.: Reference surfaces of the planet mercury from messenger. Icarus **264**, 239–245 (2016)
Lari, G.: A semi-analytical model of the Galilean satellites' dynamics. Celest. Mech. Dyn. Astron. **130**(8), 50 (2018)
Lari, G., Schettino, G., Serra, D., Tommei, G.: Orbit determination methods for interplanetary missions: development and use of the orbit14 software. Exp. Astron. **53**(1), 159–208 (2022)
Murray, C.D., Dermott, S.F.: Solar System Dynamics. Cambridge University Press, Cambridge (1999)
Noyelles, B., Frouard, J., Makarov, V.V., Efroimsky, M.: Spin–orbit evolution of mercury revisited. Icarus **241**, 26–44 (2014)
Ragazzo, C., Boué, G., Gevorgyan, Y., Ruiz, L.S.: Librations of a body composed of a deformable mantle and a fluid core. Celest. Mech. Dyn. Astron. **134**(2), 10 (2022)
Rochester, M.G.: In: Mansinha, L., Smylie, D.E., Beck, A.E. (eds.) Core–Mantle Interactions: Geophysical and Astronomical Consequences, pp. 136–148. Springer, Dordrecht (1970). https://doi.org/10.1007/978-94-010-3308-4_13
Scoppola, B., Troiani, A., Veglianti, M.: Tides and dumbbell dynamics. Regul. Chaotic Dyn. **27**(3), 369–380 (2022a)
Scoppola, B., Troiani, A., Veglianti, M.: Shaken dynamics on the 3d cubic lattice. Electron. J. Probab. **27**, 1–26 (2022b)
Showman, A.P., Stevenson, D.J., Malhotra, R.: Coupled orbital and thermal evolution of Ganymede. Icarus **129**(2), 367–383 (1997)
Smith, D.E., Zuber, M.T., Phillips, R.J., Solomon, S.C., Hauck, S.A., Lemoine, F.G., Mazarico, E., Neumann, G.A., Peale, S.J., Margot, J.-L., et al.: Gravity field and internal structure of mercury from messenger. Science **336**(6078), 214–217 (2012)
Williams, J.G., Boggs, D.H., Yoder, C.F., Ratcliff, J.T., Dickey, J.O.: Lunar rotational dissipation in solid body and molten core. J. Geophys. Res. Planets **106**(E11), 27933–27968 (2001)
Zubarev, A., Nadezhdina, I., Oberst, J., Hussmann, H., Stark, A.: New Ganymede control point network and global shape model. Planet. Space Sci. **117**, 246–249 (2015)